

# Fast and Blind Speech Copy-Move Detection and Localization in Noise

Dong Yang, Mingle Liu, Muyong Cao

**Abstract**—Copy-move forgery on speech (CMF), coupled with post-processing techniques, presents a great challenge to the forensic detection and localization of tampered areas. Most of the existing CMF detection approaches necessitate pre-segmentation of speech to facilitate similarity calculations among these segments. However, these approaches usually suffer from the problems of uncontrollable computational complexity and sensitivity to the presence of a word that is read multiple times within a speech recording. To address these issues, we propose a local feature tensors-based CMF detection algorithm that can transform duplicate detection and localization problems into a special tensor-matching procedure, accompanied by complete theoretical analysis as support. Through extensive experimentation, we have demonstrated that our method exhibits computational efficiency and robustness against post-processing techniques. Notably, it can effectively and blindly detect tampered segments, even those as short as a fractional second. These advantages highlight the promising potential of our approach for practical applications.

**Index Terms**—Speech forensics, blind detection, copy-move detection, local feature tensors

## I. INTRODUCTION

COPY-MOVE forgery speech is often imperceptible to human beings due to its derivation from real prerecorded recordings and manipulation using sophisticated audio editing tools. Furthermore, speech recordings in everyday life can be lengthy, while the tampered parts within a recording may be sparse in time. Hence, detecting CMF through auditory and visual analysis becomes challenging. Additionally, post-processing manipulations, including filtering, compression, resampling, and even the presence of background noise and music, further complicate the detection process.

In recent years, scholars have shown a growing interest in speech forensics, resulting in numerous reported works in this field [1]. Most of the existing forgery detection techniques can be broadly classified into active and passive techniques. Passive techniques [2] [3] are considered more practical because they verify the authenticity of audio by analyzing its contents and structure. Q. Yans et al [4] [5] proposed an acoustic features similarities-based CMFs detecting method. F. Wang et al [6] presented discrete cosine transforms and singular value decomposition techniques. Z. Liu et al [7] discussed the Pearson correlation coefficient (PCC) based method in the discrete Fourier transform (DFT) domain

to verify the similarity of the speech segments and M. Imran et al [3] compare the histograms computed via 1-D local binary pattern operator to identify locations of CMF. The main drawbacks of the existing CMF detection methods can be summarized as follows:

1) These methods usually assume that the speech recording has sufficient between-utterance silence [3] [4] [8] [5] [9] [10]. However, in real conversation scenarios, it is evident that this assumption does not hold, and thus they are not able to perform a fully blind analysis.

2) These methods rely on similarity computation [4] [5], which leads to the need for complex thresholds tuning and tends to misjudge when a word is read multiple times within a speech recording. Additionally, their computational complexity is non-linear, making the computation time unpredictable for long recordings.

3) These methods can work well in speech recordings without or with only light post-processing, but they may be sensitive to severe post-processing attacks.

In this work, an efficient, fully blind, and robust speech anti-CMF algorithm based on local feature tensors (LFTs) that transforms duplicate detection and localization problems into a special tensor-matching procedure is proposed. The rest of this paper is organized as follows. In Section II, we first revisit the issues of speech CMF and then show the details of our proposed scheme. The experimental results are presented in Section III, followed by a conclusion in Section IV.

## II. APPROACH

### A. Framework

Fig. 1 presents the framework of our proposed speech forgery detection scheme. The search and localization of duplicated segments in the speech recordings are computed in the logarithmic STFT magnitude (LSTFTM) spectrum domain by exploring the attributes of time-frequency (T-F) spectrogram representation, namely the LFTs. The principles for designing the LFTs are that they should be temporally and frequently localized, temporally translation invariant, robust to channel interference, and sufficiently entropic. We obtain the LFTs from the harmonic constellation map (HCM) on a speech spectrogram, which can be readily incorporated into CMF identification and localization implemented by an efficient bin-wise duplication searching algorithm. In the following paragraphs, we will introduce the process of the proposed method in detail.

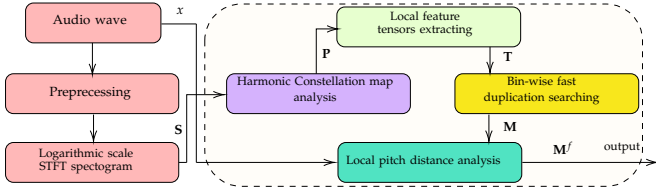


Fig. 1: Flowchart of the proposed approach

### B. Harmonic constellation map analysis (HCMA)

LSTFTM is used as a quadratic T-F representation analysis tool in speech processing. To compensate for the spectral shape, a pre-emphasis filter is initially applied to emphasize higher frequencies of the speech signal  $x$ . Finally, LSTFTM can be expressed as

$$S(t, f) = 20 \log_{10} |X(t, f)| = 20 \log_{10} |STFT\{x\}| \quad (1)$$

A point  $(i, j)$  on the spectrogram  $S = \{S(t, f)\}$  is considered a candidate peak if it has maximal amplitude among its neighbors in a region  $B_{i,j}$ , centered around of it, with the shape of  $B$ . All these identified peaks are denoted as  $P$  and can be calculated as follows:

$$P = \{(i, j) \mid S(i, j) \geq S(i', j'), \forall (i', j') \in B_{i,j}\} \quad (2)$$

We choose spectrogram peaks as key points, due to their robustness in the presence of background noise [11]. However, selecting a dense neighborhood (DNB)  $B_d$ , such as a rectangle shape  $B_d = [h, d]$ , leads to sparser and more scattered peaks, as illustrated in Fig 2b. Considering the harmonic characteristics of voiced speech, opting for a sparse neighborhood (SNB)  $B_s$  yields a higher count of peaks along the harmonics curves on the spectrogram. This effect is particularly evident in the rapidly changing portion of the harmonics over time, as shown in Fig. 2c. Due to the typically higher transient speech energies along the harmonic curves, selecting an SNB enhances robustness against noise. Moreover, the harmonics on the spectrogram exhibit smooth curves over time, leading to a more harmonically structural pattern of peaks. Consequently, it increases the presence of valid spectrogram peaks. To effectively capture the variations in the slope of the harmonic curves on the spectrogram, we devise an SNB in the shape of a flat cross with parameters  $B_s = [h_1, h_2, d, d_1]$ . Fig. 2a presents a conceptual illustration and comparison of the peak detection scheme, showing the differences between the rectangle and flat cross neighborhoods. In the figure, the SNB, with an equivalent scale of the receptive field, demonstrates superior tracking of local peaks on harmonics compared to the DNB. This sparse approach also effectively avoids false peaks resulting from noise interference between harmonics. Among the parameters of the  $B_s$ , the parameter  $h_2$  controls the capturing of the magnitude information between harmonics along the frequency axis. Parameter  $h_1$  controls the capturing of the magnitude information on the harmonics and regulates the sampling interval for peak detection along the time axis. Assuming we know the fundamental

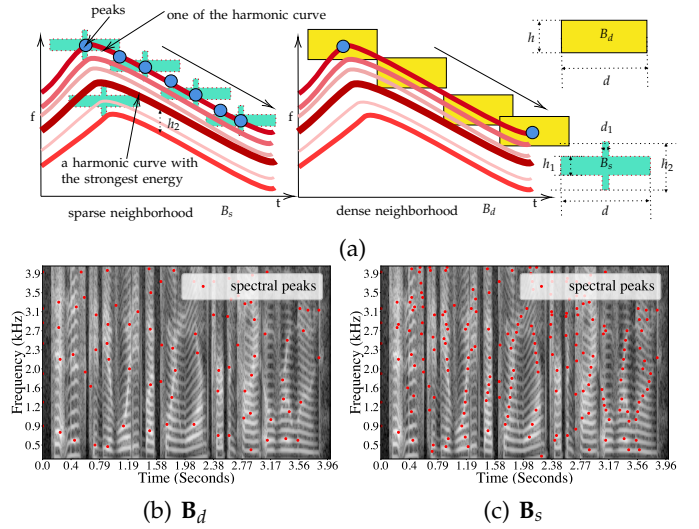


Fig. 2: (a) Comparison of the peak detection scheme with DNB and SNB on harmonics. (b) and (c) peak detection on the spectrogram with DNB and SNB respectively.

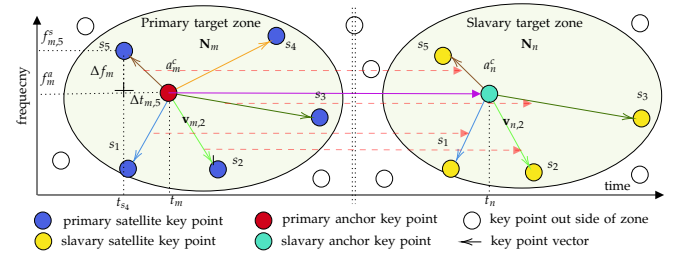


Fig. 3: Illustration of the LFTs extracting scheme, where LFTs are generated with anchors at time  $t_m$  and  $t_n$  and an example of matching the pair of the LFTs ( $T_m, T_n$ ).

frequency  $F_0$ , sampling rate  $R$  and FFT size  $L$ , a good choice for  $h_2$  can be  $\frac{2F_0L}{R}$ .

### C. Local feature tensors extracting

In this stage, LFTs of the speech signals are computed based on the HCMA. Initially, the  $m$ -th anchor  $a_m = (f_m^a, t_m) \in P$  and a target zone  $N_m$  centered around  $a_m$  are identified on the HCM. Then the anchor  $a_m$  is sequentially paired with the  $l$ -th satellite peak  $s_l = (f_{m,l}^s, t_{s_l})$  within  $N_m$ , as depicted in Fig. 3, yielding a vector consisting of two frequency components plus the time difference between them  $\Delta t_{m,l}$ , written as  $\mathbf{v}_{m,l} = [f_m^a, f_{m,l}^s, \Delta t_{m,l}]$ , which is temporally translation invariant. We define  $\mathbf{V}_m = \{\mathbf{v}_{m,l}\}$ , extended vector  $\mathbf{V}_m^e = \{[\mathbf{v}_{m,l}, t_m]\}$  and  $\mathbf{V}^e = \{\mathbf{V}_m^e\}$  that contains the absolute timestamps of the anchors so that we can later retain the duplicate time offset. It is assumed that fan-out number  $F_m = \text{card}(\mathbf{V}_m)$ . To ensure manageable computational complexity, the number of elements of  $\mathbf{V}_m$  is limited to  $F$  by discarding the excess elements.  $f_m^a$  and  $f_{m,l}^s$  are integers less than half of FFT-size  $L/2$ , and the range of  $\Delta t_{m,l}$  is also limit in the size of target zone along the time axis, denoted by  $N_x$ , and thus  $\mathbf{v}_{m,l}$

can be embedded to an integer  $z_{m,l}$  without information loss as follows:

$$z_{m,l} = 2^{(L/2 + \lceil \log_2 N_x \rceil)} f_m^a + 2^{(\lceil \log_2 N_x \rceil)} f_{m,l}^s + \Delta t_{m,l} \quad (3)$$

The count of  $z_{m,l}$  per second is approximately equal to the density of peaks  $\kappa$  times the fan-out number  $F$  in the target zone. The value of  $\kappa$  generally depends on the size and geometry of  $\mathbf{B}$ . In order to further reduce the computational complexity, we will eliminate these candidates who have no duplication in  $\mathbf{V}^e$  as they are not related to the copy-move operation. This is achieved in (4) by fast hashing duplicate elimination method [12] on  $\mathbf{z}$ , which has complexity in order of  $O(\lfloor \kappa F T_s \rfloor)$ .

$$\mathbf{u}_m = \{\mathbf{v}_{m,l}^e \in \mathbf{V}^e \mid z_{m,l} = z_{i,j}, \forall m \neq i, l \neq j\} \quad (4)$$

Here  $T_s$  is the duration of the recording. We define LFTs  $\mathbf{T} = \{\mathbf{u}_m \neq \emptyset\}$ . With  $\mathbf{T}$ , we refresh the anchor points into a more compact version  $\mathbf{A}_c$  by deleting the redundant candidates that  $\mathbf{u}_m = \emptyset$ . Up to this step, we have greatly increased the entropy of features by using  $\mathbf{T}$  instead of  $\mathbf{V}^e$ . An illustration of a local feature tensor  $\mathbf{T}_m$  centered at  $a_m^c \in \mathbf{A}_c$  in target zone  $\mathbf{N}_m$  is shown in Fig. 3.

#### D. Bin-wise fast duplication searching

If the number of element in  $\mathbf{T}_m \cap \mathbf{T}_n$  is greater than  $k$ , we consider that there is suspected duplication between  $a_m^c$  and  $a_n^c$ , where  $k$  is small integer. As it shows in Fig. 3, if select  $k=3$ ,  $a_m^c = (f_m^a, t_m)$  and  $a_n^c = (f_n^a, t_n)$  are the pairs of matched anchors as it has four vectors matched. Particularly, we notice that these two matched anchors must share the same frequency bin  $f_m^a$  since duplication is expected to be frequency invariant. Therefore the process of  $\mathbf{T}_m \cap \mathbf{T}_n$  can be simplified by considering only the frequency axis.

$$\mathbf{M} = \{(m, n) \mid f_m^a = f_n^a, \text{card}(\mathbf{T}_m \cap \mathbf{T}_n) \geq k\} \quad (5)$$

At the same time, since  $\mathbf{T}_m$  and  $\mathbf{T}_n$  contain absolute timestamps, we can readily obtain the specific time positions of anchor  $m$  and  $n$  through the inverse operation of (3). Suppose it has total  $N_a$  anchors, along the frequency axis, the computational complexity is reduced from  $O(FN_a^2)$  to  $O(FN_a^2/L)$ . Typically, when the audio is sufficiently long, indicating that  $N_a \gg F$ , and usually  $k \leq 3$ , by employing fast hashing duplication searching, the computational complexity is ultimately reduced to  $O(N_a F^k / L)$ , resulting in linear complexity. Specifically, if the CMF is sparse in audio,  $N_a$  can be negligible.

Let us assume  $p$  is the probability of a peak surviving in a noise attack. It generally is monotonic increasing with the signal-to-noise ratio (SNR). Considering the event  $E_m^a = \{0, 1\}$  and  $E_n^a = \{0, 1\}$  representing the survival of the anchors  $a_m^c$  and  $a_n^c$ , if the entire speech is attacked by noise, the probability of both of the anchors can survive is given by  $p_2^a = P(E_m^a \wedge E_n^a = 1) = p^2$ . Consequently, the probability of duplication that there are  $k$  or more matched pairs of vector  $(\mathbf{v}_{m,l}, \mathbf{v}_{n,l})$  is as follows:

$$P_d(k) = \sum_{E_m^a, E_n^a} P_d(k, E_m^a, E_n^a) = p_2^a P_d(k \mid E_m^a \wedge E_n^a = 1) \quad (6)$$

Similar to the anchor pairs, the matched satellites have three possible states, and the probability of the state of each pair  $(E_m^{s_l}, E_n^{s_l})$  can be expressed as follows:

$$\begin{aligned} p_2^s &= P(E_m^{s_l} \wedge E_n^{s_l} = 1) = p^2 \\ p_1^s &= P(E_m^{s_l} \oplus E_n^{s_l} = 1) = 2(1-p)p \\ p_0^s &= P(E_m^{s_l} \vee E_n^{s_l} = 0) = (1-p)^2 \end{aligned} \quad (7)$$

Assuming that the satellites around the anchors are independent and identically distributed (IID), finally (6) is boiled down to the sum of combinations given by

$$P_d(k) = p_2^a \sum_{i=k}^F C_F^k (p_2^s)^k \left[ \sum_{i=0}^{F-k} C_k^i (p_1^s)^i (p_0^s)^{F-k+i} \right] \quad (8)$$

In a simpler scenario where the primary tensor is from known audio and only the duplicate counterpart is attacked by noise, we have  $P(E_m^a \wedge E_n^a = 1) = P(E_n^a = 1) = p$ . Accordingly, (6) degenerates to

$$P_d(k) = p P(k \mid E_n^a = 1) = p \sum_{i=k}^F C_F^i p^i (1-p)^{F-i} \quad (9)$$

Finally, the probability of at least one pair of tensors existing in the speech, which represents the recall of detection, can be formulated as follows:

$$P_{exist} = 1 - (1 - P_d(k))^{\frac{\mathbb{E}(M)}{2}} \quad (10)$$

where  $M$  represents the number of anchors in  $\mathbf{A}_c$ , and its expected value is given by  $\mathbb{E}(M) = 2P_d(k=1) \kappa T_d$ .  $T_d$  is the duration of duplication. As long as  $\kappa T_d$  is sufficiently large, the duplication is easily found.

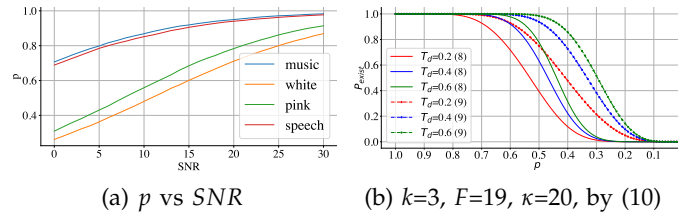


Fig. 4: (a) Comparison of  $p$  vs SNR for various types of noise. (b) results of  $P_{exist}$  vs  $p$  applying with (8) and (9) respectively for various different of  $T_d$ .

#### E. Local pitch distance analysis

To further minimize the residual accidental false alarms, we devised the dynamic time warping [13] pitch distance factor (DTW-PDF) between two matched anchors to assess the confidence of the duplication by (5). If we set threshold  $\theta$ , duplication finally is confirmed by

$$\mathbf{M}^f = \{(m, n) \mid DTW_e(\mathbf{P}_m^D, \mathbf{P}_n^D) / C_b \leq \theta\}. \quad (11)$$

where  $C_b$  refers to the confidence boundary, which represents the maximum acceptable standard deviation for pitch estimation. The pitch slice is defined as  $\mathbf{P}_m^D = \mathbf{P}_s(m-D : m+D)$ . Pitch sequence  $\mathbf{P}_s$  can be estimated using REAPER [14] [15]. Due to potential inconsistencies in pitch estimation, the effective lengths of the

$\mathbf{P}_m^D$  and  $\mathbf{P}_m^D$  may not be necessarily aligned. To address this, we employ Euclidean distance-based dynamic time warping (DTW) operator,  $DTW_e$ , to handle the situation.

### III. PERFORMANCE EVALUATION

In this work, the TIMIT speech database [16] was used to generate test copy-move datasets, which contain a total of 6300 sentences. Multiple sentences are randomly concatenated to a speech restricted between 12 and 60 seconds. For each speech recording, a segment of fixed duration is randomly selected and then randomly copied to another location within the same speech. The duration of duplication  $T_d$  ranges from 0.2 to 1.0 seconds. The positive and negative samples are evenly distributed in the dataset. Precision and recall were used to measure the performance of the proposed method. We employ FFT size  $L=512$  along with a hanning window of length  $L_w=512$ , and hop length  $H=64$  for STFT. Fundamental frequency  $F_0$  is estimated by REAPER [14]. Parameters of  $\mathbf{B}_s = [3, \max(8, \frac{2F_0L}{R}), 15, 1]$ ,  $\mathbf{B}_d = [8, 15]$ ,  $k=3$ ,  $F=19$ ,  $C_b=10$  (Hz),  $D=5$ , and threshold  $\theta = 0.5$ . The target zone  $\mathbf{N}_m = \{(i, j) \mid |i - i'| \leq \frac{N_x}{2}, 0 \leq j \leq \frac{L}{2}\}$  is a rectangle centered at  $a_m^c = (i', j')$  and  $N_x = 40$ . Our method achieves 0.008 real-time factor on a 2.6 GHz Intel i7 core implemented using Python3.8.

Fig 4b shows the effect of surviving probability  $p$  on  $P_{exist}$  for various choose of  $T_d$ . In connection with Fig 4a, under the same SNR, steady-state noise such as white noise has a greater impact on performance than transient noise. Therefore, we generate the copy-move forged speech datasets with additive white noise. The experimental results of our proposed method demonstrate comparable average precision, achieving 99.70% and 99.68% using DNB and SNB, respectively. Fig. 5 shows the recall at various SNR levels for both cases using DNB and SNB. When selecting an SNB, the performance significantly exceeds its dense counterpart. By comparing Fig. 5a, Fig. 5b and Fig 4b, the overall trend is consistent with formula (10) because when a DNB is chosen, the distribution of peaks is sparser and more in line with the IID assumption in (8). In contrast, employing an SNB leads to an increased number of valid anchors  $M$ , along with the survival probability  $p$  at a lower SNR. Additionally, these peaks possess a more harmonically structural pattern and mutual dependency. Consequently, this ultimately yields improved performance according to (10). Tab. I shows our method also demonstrates robustness against compression degradation at low bit rates, filtering, and resampling attacks.

To fairly compare with other methods, five types of common post-processing operations [17] are chosen to attack, including MP3 degradation, Gaussian noise with SNR=10dB and 20dB respectively, resampling, and filtering. LibriSpeech [18] and Chinspeech [17] are used to generate test datasets as the same procedure in [17]. Tab.II presents the overall performance across five types of anti-forensics attacks, indicating that our method generally outperforms the methods proposed by Yan [5] and

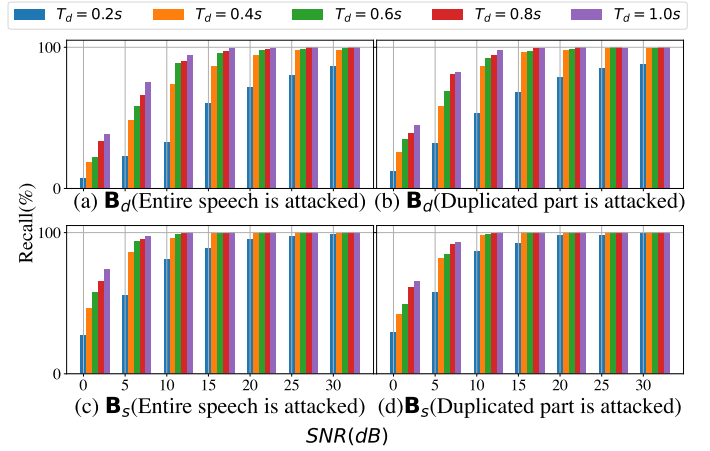


Fig. 5: The performance for the cases of entire speech and only duplicated parts under white noise attack at different SNR levels for various duplicate duration  $T_d$ . (a) and (b) recall using  $\mathbf{B}_d$ . (c) and (d) recall using  $\mathbf{B}_s$ .

Z. Yang's CQSS-299 [17]. Particularly, Yan's method or similar approaches are not competitive primarily due to their reliance on the assumption of between-utterance silence for speech segmentation, which is not suitable for real-world applications.

TABLE I: Performance (%) under different anti-forensics attacks using  $\mathbf{B}_s$  for various  $T_d$ .

Codecs	Recall					Precision
	0.2	0.4	0.6	0.8	1.0	
PCM	98.58	100.0	100.0	100.0	100.0	99.24
MP3(32k)	97.87	100.0	100.0	100.0	100.0	99.59
Opus(6k)	97.48	100.0	100.0	100.0	100.0	99.98
Lowpass [19]	98.55	100.0	100.0	100.0	100.0	99.48
Resampling	98.43	100.0	100.0	100.0	100.0	99.48

TABLE II: Average Performance (%) under five types of anti-forensics attacks.

Methods	LibriSpeech			ChinSpeech		
	Yan	CQSS-299	Ours	Yan	CQSS-299	Ours
Precision	85.6	97.1	<b>99.5</b>	88.8	99.4	<b>99.7</b>
Recall	81.0	97.2	<b>98.3</b>	90.1	97.0	<b>96.8</b>

### IV. CONCLUSION

In this letter, a new CMF detection and location method is proposed based on comparing the local tensor features. Different from previous works, we truly achieve fully blind and continuous analysis by inspecting the T-F structure of a speech recording without relying on any speech priors and segmentation. Our theoretical analysis demonstrates it performs effective and efficient speech CMF detection and localization in linear complexity. Via extensive experiments and comparisons, we validate the effectiveness of the proposed method, which is robust against various post-processing attacks.

## REFERENCES

- [1] P. R. Bevinamarad and M. S. Shirdonkar, "Audio forgery detection techniques: Present and past review," *2020 4th International Conference on Trends in Electronics and Informatics (ICOEI)*(48184), pp. 613–618, 2020.
- [2] H. Zhao, Y. Chen, R. Wang, and H. Malik, "Audio source authentication and splicing detection using acoustic environmental signature," in *Proceedings of the 2nd ACM workshop on Information hiding and multimedia security*, 2014, pp. 159–164.
- [3] M. Imran, Z. Ali, S. T. Bakhsh, and S. Akram, "Blind detection of copy-move forgery in digital audio forensics," *IEEE Access*, vol. 5, pp. 12 843–12 855, 2017.
- [4] Q. Yan, R. Yang, and J. Huang, "Robust copy-move detection of speech recording using similarities of pitch and formant," *IEEE Transactions on Information Forensics and Security*, vol. 14, no. 9, pp. 2331–2341, 2019.
- [5] —, "Copy-move detection of audio recording with pitch similarity," in *2015 IEEE International Conference on Acoustics, Speech and Signal Processing (ICASSP)*, 2015, pp. 1782–1786.
- [6] F. Wang, C. Li, and L. Tian, "An algorithm of detecting audio copy-move forgery based on dct and svd," in *2017 IEEE 17th International Conference on Communication Technology (ICCT)*. IEEE, 2017, pp. 1652–1657.
- [7] Z. Liu and W. Lu, "Fast copy-move detection of digital audio," *2017 IEEE Second International Conference on Data Science in Cyberspace (DSC)*, pp. 625–629, 2017.
- [8] F. Akdeniz and Y. Becerikli, "Linear prediction coefficients based copy-move forgery detection in audio signal," in *2022 International Symposium on Multidisciplinary Studies and Innovative Technologies (ISMSIT)*, 2022, pp. 770–773.
- [9] Z. Liu and W. Lu, "Fast copy-move detection of digital audio," in *2017 IEEE Second International Conference on Data Science in Cyberspace (DSC)*, 2017, pp. 625–629.
- [10] Z. Xie, W. Lu, X. Liu, Y. Xue, and Y. Yeung, "Copy-move detection of digital audio based on multi-feature decision," *Journal of Information Security and Applications*, vol. 43, pp. 37–46, 2018. [Online]. Available: <https://www.sciencedirect.com/science/article/pii/S2214212617304404>
- [11] A. Wang *et al.*, "An industrial strength audio search algorithm." in *Ismir*, vol. 2003. Washington, DC, 2003, pp. 7–13.
- [12] C. E. Leiserson, R. L. Rivest, T. H. Cormen, and C. Stein, *Introduction to algorithms*. MIT press Cambridge, MA, USA, 1994, vol. 3.
- [13] P. Senin, "Dynamic time warping algorithm review," 2008. [Online]. Available: <https://api.semanticscholar.org/CorpusID:16629907>
- [14] D. Talkin, "Reaper: Robust epoch and pitch estimator," *GitHub*: <https://github.com/google/REAPER>, 2015.
- [15] D. Jouviet and Y. Laprie, "Performance analysis of several pitch detection algorithms on simulated and real noisy speech data," in *2017 25th European Signal Processing Conference (EUSIPCO)*, 2017, pp. 1614–1618.
- [16] J. Garofolo, L. Lamel, W. Fisher, J. Fiscus, D. Pallett, and N. Dahlgren, "Darpa timit acoustic-phonetic continuous speech corpus cd-rom TIMIT," 1993-02-01 1993.
- [17] Z. Su, M. Li, G. Zhang, Q. Wu, M. Li, W. Zhang, and X. Yao, "Robust audio copy-move forgery detection using constant q spectral sketches and ga-svm," *IEEE Transactions on Dependable and Secure Computing*, pp. 1–15, 2022.
- [18] V. Panayotov, G. Chen, D. Povey, and S. Khudanpur, "Librispeech: An asr corpus based on public domain audio books," in *2015 IEEE International Conference on Acoustics, Speech and Signal Processing (ICASSP)*, 2015, pp. 5206–5210.
- [19] L. Milic, S. Damjanovic, and M. Nikolic, "Frequency transformations of iir filters with filter bank applications," in *APCCAS 2006 - 2006 IEEE Asia Pacific Conference on Circuits and Systems*, 2006, pp. 1051–1054.